Spin-$\frac{1}{2}$ frustrated Heisenberg model at finite temperature

S. Bacci, E. Gagliano, and E. Dagotto*
Physics Department and Material Research Laboratory, University of Illinois at Urbana-Champaign, 1110 West Green Street, Urbana, Illinois 61801
(Received 11 October 1990; revised manuscript received 20 February 1991)

We analyzed the thermodynamic properties of the two-dimensional spin-$\frac{1}{2}$ frustrated antiferromagnetic Heisenberg model. Using a Lanczos-like technique to avoid the diagonalization of the complete Hamiltonian matrix, we calculate the specific heat, uniform susceptibility, structure factor, and dimer susceptibility for different values of the frustration parameter, J_2/J_1. At low temperatures and intermediate values of J_2/J_1, the enhancement of the column correlation function shows that in this regime the dimer state may be the ground state. Although the behavior of the magnetic structure factor at $J_2/J_1 \approx 0.5$ can be roughly described by a dimer state, this kind of state cannot explain an observed quasidegeneracy at $J_2/J_1 \approx 0.6$ of the values of the structure factor between $\mathbf{q}=(\pi,\pi)$, $(0,\pi)$, and $(\pi/2,\pi)$. We also calculated the twisted susceptibility at nonzero momentum. For $\mathbf{q}=(0,\pi/2)$ we found an enhancement of a factor 2 at $J_2/J_1 \approx 0.6$ with respect to the infinite-temperature limit.

I. INTRODUCTION

Following the discovery of the oxide superconductors,[1] the interest in two-dimensional quantum spin systems has been renewed, mainly due to the possibility that superconductivity in the CuO_2 layers may be related to their magnetic properties.[2] Although the CuO_2 layers have both Cu and O orbitals, it has been suggested that for a realistic set of parameters, the high-T_c materials may be described by a two-dimensional (2D) one-band Hubbard model. In the strong Coulomb limit, and at half-filling, this model can be further simplified to a spin system. In this way, an effective spin-$\frac{1}{2}$ antiferromagnetic Heisenberg model (AFH) on the square lattice has been proposed to describe the undoped compound.[3] The rich magnetic structure experimentally observed in La_2CuO_4 seems to be qualitatively described by this effective model.

Unfortunately, the situation for the doped case is less clear. The kinetic part of the Hubbard Hamiltonian can be considered under several approximations leading to different effective Hamiltonians. In one of these proposals, it is assumed that at a small density of carriers, the holes can be integrated out yielding an effective spin Hamiltonian, which is an antiferromagnetic Heisenberg model with frustration (FAFH).[4] The frustration is introduced through an additional next-nearest-neighbor coupling along the diagonal of the plaquettes of the lattice. Although the validity of these approximations is questionable, the FAFH is an important model by itself, since event the pure AFH has played a significant role in the understanding of the magnetic properties of solids. In this paper, we study the thermodynamic properties of the spin-$\frac{1}{2}$ FAFH, defined by the Hamiltonian

$$H = J_1 \sum_{\mathbf{i},\hat{\epsilon}} \mathbf{S}_\mathbf{i}\cdot\mathbf{S}_{\mathbf{i}+\hat{\epsilon}} + J_2 \sum_{\mathbf{i},\hat{\delta}} \mathbf{S}_\mathbf{i}\cdot\mathbf{S}_{\mathbf{i}+\hat{\delta}} \,. \quad (1)$$

Here, $\mathbf{i}$ denotes the sites of a square lattice, while $\hat{\epsilon}$ are vectors along the x or y directions, and $\hat{\delta}$ along the diagonal of the plaquettes. $\mathbf{S}_\mathbf{i}$ are spin-$\frac{1}{2}$ operators. We use periodic boundary conditions and the energy scale is fixed as $J_1 = 1$.

The model at $J_2 = 0$ is well understood. At $T=0$ and in the limit $S \to \infty$, the spins are classical vectors, and the ground state is the Néel state. At $S=\frac{1}{2}$, the quantum fluctuations are strong enough to reduce the staggered magnetization from its classical value $m=0.5$ to $m \approx 0.31$. This finite value shows the existence of long-range order. This result is strongly supported by numerical calculations.[5] However, as predicted by the Mermin-Wagner theorem,[6] long-range order cannot exist for the 2D Heisenberg model at finite temperature. In the classical limit of the FAFH model, the next-nearest-neighbor coupling J_2 acts against the Néel order, which, nevertheless, is not completely destroyed for small J_2. For $J_2/J_1 > 0.5$, J_2 is large enough to destroy the sublattice magnetization, resulting in two decoupled Néel sublattices in the classical limit. These two sublattices are coupled only when quantum fluctuations are introduced.

At $T=0$, the spin-$\frac{1}{2}$ FAFH model has been analytically studied using several techniques. The ground-state properties have been analyzed by a spin-wave approach,[7] $1/N$ expansion,[8] and series expansion around dimerized Hamiltonians.[9] These studies show that at a certain value of the frustration interaction, $J_2/J_1 \approx 0.5$, quantum fluctuations are strong enough to destroy the Néel order, but they are in disagreement about the nature of the intermediate phase. Several proposals have been made for the ground state in this region, including a spin-liquid state (no broken symmetries),[7] a spontaneously column-dimerized state,[8] twisted,[10] and chiral order.[11] The static properties of the ground state and excited states have been studied using the Lanczos algorithm and by exact diagonalization in finite clusters.[12,13] At large J_2, it was

found[12] that the ground state is the collinear state (configurations that have alternating rows, or columns, of spins up or down). This state does not have the full symmetries of the lattice, since the horizontal and vertical "strip" states are connected by a lattice rotation of $\pi/2$. Based on the $T=0$ behavior of zero-momentum correlation functions, at intermediate values of J_2/J_1, both dimers or twisted states were found to be possible candidates.[12] Since exact diagonalization or Lanczos techniques must deal with the complete Hilbert space, its rapid increase in dimension with the number of sites restricts the size of the clusters that can be handled. On the other hand, a phase transition is only possible for an infinite system, i.e., when an infinite number of degrees of freedom is considered. Then, to extract a conclusion from finite lattice studies, one should try to compare the behavior of the order parameters for different lattice sizes. In Ref. 12, three clusters of sizes $N=8$, 16, and 20 were considered. The clusters $N=8$ and 20 are tilted squares, which belong to the general class defined by $N=l^2+k^2$ sites, with $l+k$ even. Nevertheless, unlike the $N=16$ case, where the ground state is always even under the space-group symmetry operations, for $N=20$, a change in the symmetry of the ground state was observed as J_2/J_1 is increased, changing from even to odd under rotations. This fact complicates the extrapolation to the bulk limit. Indeed, this nonuniform behavior can be expected, since it has been shown that for the square lattice, the pure Heisenberg model has different ground-state symmetries if the number of sites is $N=4n\,(A_1)$ or $N=4n+2(B_1)$, where A_1 or B_1 label two of the irreducible representations of the C_{4v} group.[14] Since, at large J_2/J_1, the system is decoupled in two almost independent sublattices, this means that in the $N=20$ case, each one will contain $(N/2)=10$, i.e., belongs to the class $N=4n+2$ with $n=2$, and so the ground state will be odd under rotations in $(\pi/2)$. This explains the puzzling crossing of levels found in previous studies.[12] On the other hand, for large J_2/J_1, the $N=16$ case will decouple in two sublattices with $8=4n$ $(n=2)$ sites in each one, and so the symmetry of the ground state will remain unchanged over the complete range of the frustration parameter J_2/J_1. Then, we arrive at the conclusion that the next cluster to be studied in order to perform a reasonable finite size scaling contains $N=32$ sites. While the properties at zero temperature can be obtained with present Lanczos methods,[15] the calculation at finite temperature would be very difficult. The size of the Hilbert space of the $N=32$ lattice is approximately 1.2 million states after translations, rotations, reflections in one axis, and spin-inversion symmetries are used. Thus, the numerical effort to study the thermodynamic properties of this lattice would require performing 1.2 million times a calculation equivalent to that needed to obtain the ground-state properties (using the technique described in this paper) or diagonalizing matrices of size $(1.2\times10^6)\times(1.2\times10^6)$, which is impossible with present-day supercomputers.

To completely characterize the model, we need not only to study the static properties at $T=0$, but, also, to calculate the dynamical properties[16] as well as to analyze the behavior of the model at finite temperature,[17] which is the main goal of the present work. To analyze the thermodynamic properties of the FAFH model, we have used a Lanczos-like algorithm.[18] Below, we briefly describe the method and present our results.

II. NUMERICAL METHOD

Contrary to what happens with Monte Carlo methods, where nonpositive weights can be generated, the method we have used can be applied to any quantum many-body system of moderate size. It directly provides the partition function, from which all the thermodynamic quantities of interest are obtained by differentiation. The strategy is based on the introduction of the resolvent operator for H. The partition function, $Z=\mathrm{Tr}\exp(-\beta H)$, can be evaluated by rewriting it as

$$Z=\sum_i z_i \ , \tag{2}$$

where

$$z_i=\sum_\nu |\langle i|\nu\rangle|^2 e^{(-\beta E_\nu)} \ . \tag{3}$$

Here, $\{|i\rangle\}$ is any orthonormal set of states [chosen as eigenvectors of the Ising part of Eq. (1)], $\{|\nu\rangle\}$ is a complete set of eigenstates of H, and E_ν denotes the energy of the $|\nu\rangle$ eigenstate. The Laplace transform of Eq. (3), given by

$$\mathcal{L}(z_i)=\langle i|(s+H)^{-1}|i\rangle \ , \tag{4}$$

is a resolvent operator $G_i(s)=\langle i|(s-H)^{-1}|i\rangle$, which admits a continued fraction expansion

$$G_i(s)=\frac{1}{s-a_{0,i}-(b_{1,i}^2/s-\cdots)} \ . \tag{5}$$

The set of parameters $\{a_{n,i},b_{n,i}^2\}$ are obtained using the recurrence relation of the Lanczos algorithm. Starting from an arbitrary state $|f_0\rangle=|i\rangle$, a set of orthogonal states is generated:

$$|f_{n+1}\rangle=H|f_n\rangle-a_{n,i}|f_n\rangle-b_{n,i}^2|f_{n-1}\rangle \ , \tag{6}$$

$$a_{n,i}=\langle f_n|H|f_n\rangle/\langle f_n|f_n\rangle \ , \tag{7}$$

$$b_{n,i}^2=\langle f_{n-1}|H|f_n\rangle/\langle f_{n-1}|f_{n-1}\rangle \ . \tag{8}$$

In general, only a few iterations are needed to accurately evaluate the resolvent. Then, calculating $G_i(s)$ for a complete set of orthonormal states $|i\rangle$, the partition function is obtained as

$$Z=-\mathcal{L}^{-1}\left[\sum_i G_i(-s)\right] \ . \tag{9}$$

Once the set of coefficients $\{a_{n,i},b_{n,i}^2\}$ is generated, the evaluation of any diagonal operator can be done without extra cost of CPU time (nondiagonal elements need more computational effort).

The sizes and geometries of the adequate lattices to study are those that keep the main symmetries of the whole system.[14] For this reason, we have studied the tilted square with $N=8$ (we exclude $N=10$, since, for large

J_2/J_1, the system would consist of two sublattices with an odd number of sites) and $N=16$, which has the full geometry of the square. For $N=16$, we have implemented the C_{4v} point group and spatial translations, reducing in this way the number of nonequivalent continued fractions to be evaluated. In Table I, we summarize (for $N=16$) the size of the Hilbert space for the different sectors of total spin projection and the corresponding reduction using symmetries. To double check our program, we computed the ground-state energy at $T=0$ using a modified Lanczos algorithm[19] and compared this result with the corresponding ones at finite but small temperature. The accuracy of the method is illustrated in Table II. The method we used is more efficient than the diagonalization of the Hamiltonian matrix, and since the set of coefficients obtained is temperature independent, it provides information about the whole range of temperatures. To label the basis, we use a binary code adapted for a symmetrized basis state. An important point in the finite temperature calculations is the fact that one must consider the different sectors of total spin projection, $B_0(S_z=0)$, $B_1(S_z=\pm 1)$, $B_2(S_z=\pm 2)$, and so on. Although the contributions of the higher subspaces, $B_3, \ldots,$ are negligible for the temperatures of interest, the ones coming from the B_1 and B_2 subspaces cannot be ignored. Our results have been obtained considering all the spin sectors.

TABLE I. Size of the Hilbert space for $N=16$ in each sector of total spin projection considering no symmetry reduction, only translation symmetries and the complete spatial group. The last two rows refer only to states that are not connected by symmetry operations.

Spin projection subspace, S_z	Complete base	Translation symmetry	Spatial group
±7	16	1	1
±6	120	9	5
±5	560	35	10
±4	1 820	122	33
±3	4 368	273	53
±2	8 008	511	101
±1	11 440	715	122
0	12 870	822	153

III. RESULTS

We have calculated the specific heat $C=d\langle E\rangle/dT$ and uniform magnetic susceptibility. The notation $\langle\ \rangle$ denotes the statistical average. We have calculated spin-correlation functions in momentum space. These quantities can be directly compared with neutron-scattering experiments that measure spin fluctuations in magnetic systems. Moreover, in a quantum antiferromagnet, since the Hamiltonian is symmetric under spin rotations, the staggered magnetization $m_{1,z}=(1/N)\sum_i \epsilon_i\langle S_i^z\rangle$ order parameter will be identically zero (here $\epsilon_i=\pm 1$ depending on which sublattice the site i belongs). For this reason, on a finite lattice calculation, the evaluation of $m_{1,z}$ as well as any other mean value of an operator that breaks the inherent symmetry of the Hamiltonian is not useful (unless an explicit source of symmetry breaking is introduced). Then, it is necessary to evaluate the square of a given order parameter. We have computed the structure factor,

$$S(\mathbf{q})=\frac{1}{N}\sum_{\mathrm{i,j}} e^{i\mathbf{q}\cdot(l-\mathrm{j})}\langle S_l^z S_{\mathrm{j}}^z\rangle\ , \tag{10}$$

for different values of the allowed wave vector $\mathbf{q}$ in the first Brillouin zone. The staggered magnetization m_1^2 can be obtained from the Fourier transform $S(\mathbf{q})$ of the spin-spin correlation function $m_1^2=(3/N)S(\pi,\pi)$, where $\mathbf{q}=(\pi,\pi)$ is the wave vector of the staggered magnetization. The factor of 3 appears to be due to rotational invariance. We also calculated $S(0,\pi)$, which is related with the staggered magnetization m_2^2 in the "collinear" phase at large J_2/J_1. In Fig. 1, we present $S(\pi,\pi)$ for the AFH model, showing the enhancement of this order parameter for increasing lattice size N and $T\to 0$. Although it is difficult to show it numerically, we believe that this order parameter is diverging exponentially with $1/T$ at low temperatures in the bulk limit as suggested by renormalization group studies that map the model into a classical O(3) system.

In Fig. 2, we show $S(\pi,\pi)$ and $S(0,\pi)$ for the FAFH model. As expected, for small J_2/J_1, $S(\pi,\pi)$ displays a significant growth with decreasing temperature having, at $J_2=0$, a maximum value typical of a Néel-like order, where spin fluctuations are correlated over long distances. Increasing J_2, this order parameter is suppressed, the crossover being near $J_2/J_1\sim 0.6$. On the other hand, the structure factor $S(0,\pi)$ behaves in an opposite way i.e., it increases with J_2, showing the existence of the collinear phase for $J_2/J_1>0.5$. For $T\to 0$, we reproduce the results obtained with the $T=0$ Lanczos algorithm.[12] As an illustrative example of the contribution with temperature of the different subspaces of total spin projection, we show in Fig. 3 the first three terms $S_z=0,\pm 1,\pm 2$

TABLE II. Energies for different values of J_2/J_1 at the smallest temperature studied (shown between parentheses) compared with the $T=0$ Lanczos results. The accuracy of the method is illustrated by showing the corresponding values of the computed partition function.

J_2/J_1	E_0 $(T=0)$	E $(T=5\times 10^{-3})$	Z $(T=5\times 10^{-3})$
0.10	−1.319 6343	−1.319 6341	9.456 669 008 111 048 67E+0916
0.25	−1.201 9090	−1.201 9085	1.484 648 243 661 854 33E+0835
0.50	−1.057 24	−1.057 11	3.498 029 149 476 373 39E+0.734
0.70	−1.127 716	−1.127 35	1.288 087 951 315 621 66E+0783

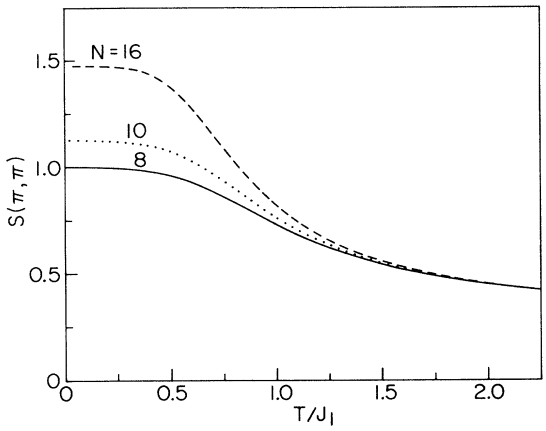

FIG. 1. Structure factor $S(\pi,\pi)$ in the Heisenberg model for different lattice sizes $N=8$, 10, and 16.

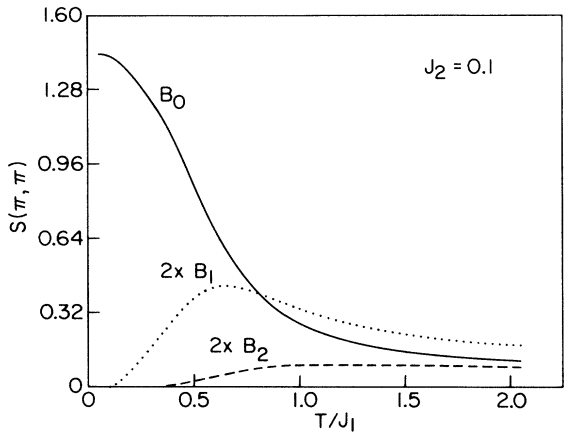

FIG. 3. The contribution to $S(\pi,\pi)$ of the first three subspaces $S_z=0(B_0),\pm1(B_1),\pm2(B_2)$ as a function of the temperature, for the FAFH with $N=16$.

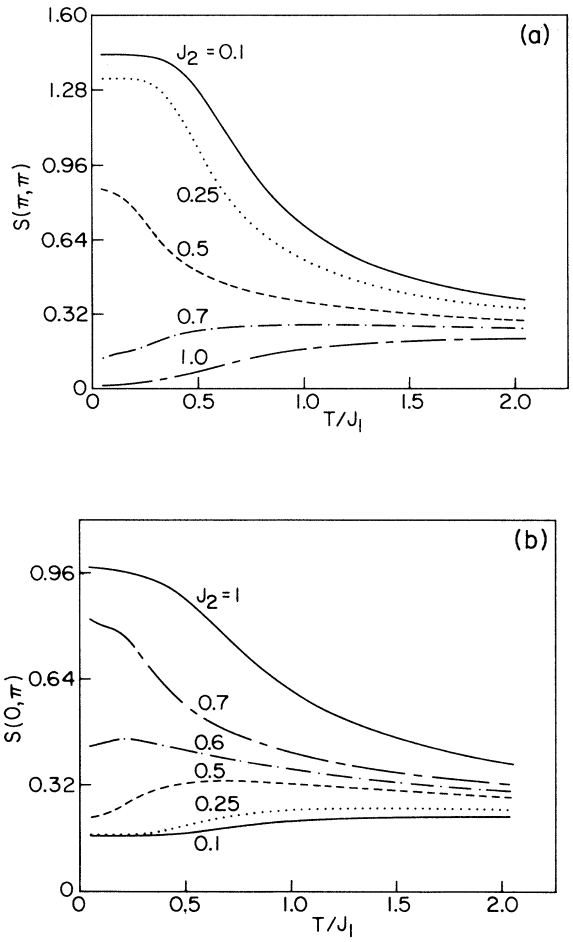

FIG. 2. Structure factor $S(\mathbf{q})$ as a function of temperature for several values of the frustration parameter J_2/J_1 and $N=16$: (a) $\mathbf{q}=(\pi,\pi)$ and (b) $\mathbf{q}=(0,\pi)$.

in $S(\pi,\pi)$ for the FAFH and $N=16$. Note that, at large temperatures, the results for all lattice sizes, J_2 couplings and $\mathbf{q}$ converges to the same number, showing that the system is completely disordered in that regimen.

The uniform susceptibility $\chi=(1/T)S(0,0)$ shows a broad maximum, both for the AFH as well as FAFH, as is illustrated in Figs. 4(a) and 4(b), respectively. At high temperatures, χ is proportional to $(1/T)$, i.e., it follows Curie's law, and so, can be approximated quite well by its high-temperature series expansion since its leading term is precisely of order $(1/T)$. In both models, the examined χ has no significant size dependence. For the AFH, there is an excellent agreement between our results and those of a Monte Carlo simulation,[20] as is shown in Fig. 4(a). Note that, at $T=0$, the uniform magnetization of a finite system vanishes since the ground state is a spin singlet for all values of J_2.

In Fig. 5, we show the specific heat C per site for the AFH model calculated from the corresponding energy data. No significant size dependence can be observed in the specific heat, and again, the comparison with Monte Carlo results[20] is very good. Here, the peak in the specific heat represents only a crossover but not a phase transition (the size dependence is very small). The position of the peak is at the inflection point of the $S(\pi,\pi)$ vs T curve. However, note that the behavior of C for the FAFH model, shown for $N=8$ and 16 in Fig. 6, is nontrivial, having a *sharpening* of the peak and a bigger size dependence at $J_2/J_1\approx0.5$, but not for other values of the frustrating parameter out of the intermediate region. The position of the peak goes through a minimum in this region. While there are clear differences between small and intermediate values of frustration, we cannot decide, studying these small lattices, whether they correspond to an actual phase transition or are just due to abrupt crossovers in the energy.

In order to study in more detail the region $J_2/J_1\approx0.5$, in which a new phase could exist, we have analyzed the possibility of a column *dimerized* state. The presence of

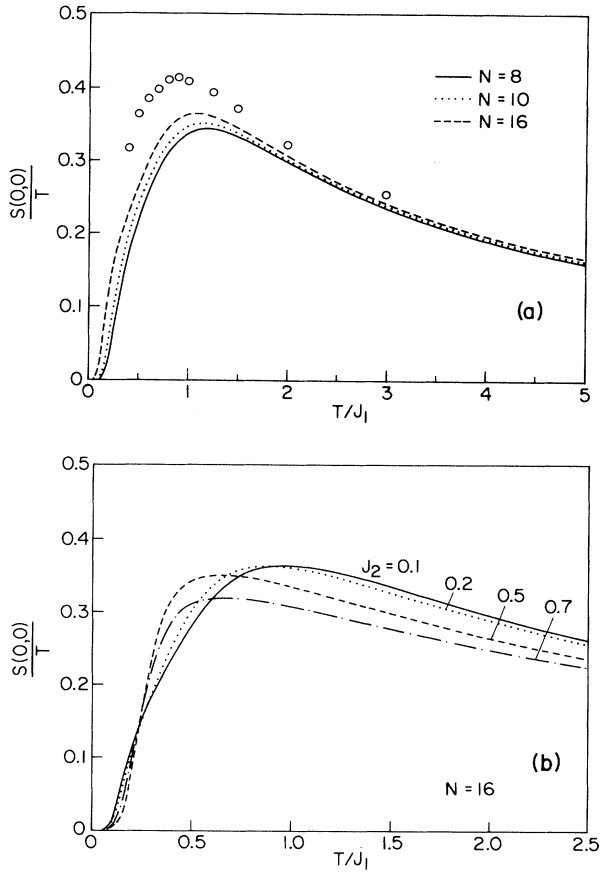

FIG. 4. Uniform susceptibility vs temperature for (a) the antiferromagnetic Heisenberg model for different lattice sizes. The open circles are MC results for 8×8 lattice, taken from Ref. 20 and (b) the FAFH for different values of the frustration parameter.

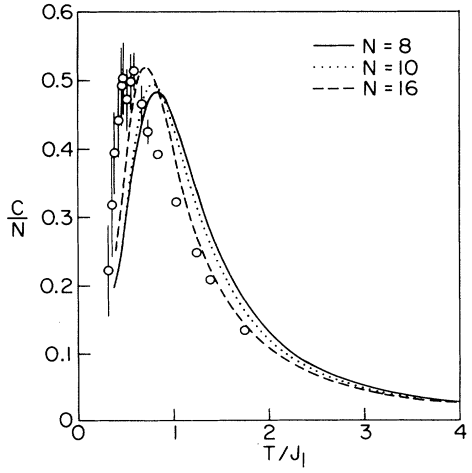

FIG. 5. Specific heat C/N for the antiferromagnetic Heisenberg model for different lattice sizes, $N=8$, 10, and 16. The open circles indicate MC results for a 12×12 lattice (taken from Ref. 20).

such a state has been tested before using the order parameter,[12]

$$\mathcal{O}_{\mathbf{i}}^{\mathrm{col}}=\eta_{\mathbf{i}}\mathbf{S}_{\mathbf{i}}\cdot(\mathbf{S}_{\mathbf{i}+\hat{\epsilon}_x}-\mathbf{S}_{\mathbf{i}-\hat{\epsilon}_x}+i\mathbf{S}_{\mathbf{i}+\hat{\epsilon}_y}-i\mathbf{S}_{\mathbf{i}-\hat{\epsilon}_y}) , \qquad (11)$$

where $\mathbf{i}$ belongs to one of the two sublattices, and $\eta_{\mathbf{i}}=\pm 1$, depending on which of the two sublattices the point belongs to. We have studied only the Ising part of $\chi^{\mathrm{col}}=\langle|(1/N)\sum_{\mathbf{i}}\mathcal{O}_{\mathbf{i}}^{\mathrm{col}}|^2\rangle$, shown in Fig. 7, since at $T=0$, we obtained similar qualitative results either considering the complete operator, Eq. (11), or only the z component of each vector. The behavior of this order parameter with temperature is in agreement with the numerical results at $T=0$ showing an enhancement of the column order. It is not yet clear if the dimer ground state survives the bulk limit (a finite size scaling will be needed using different lattices), but its behavior with J_2 and T is characteristic of an enhanced order in the intermediate region, i.e., the order parameter is large at small temperatures and then it is suppressed at high temperatures. Whether there is a phase transition at finite temperature near $J_2/J_1\sim 0.5$ cannot be decided by the present analysis. All of these results regarding the dimer state have also recently been found by Singh and Narayanan.[21]

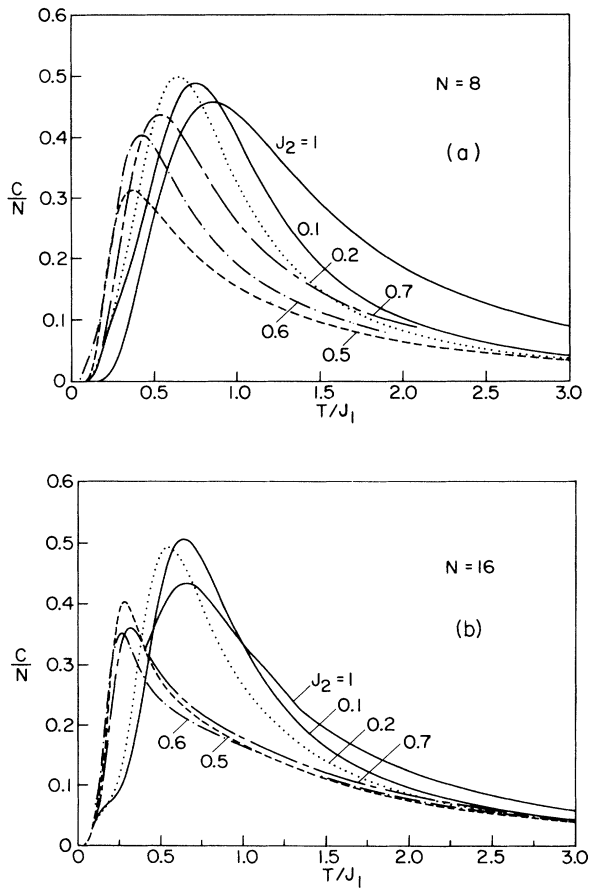

FIG. 6. Specific heat C/N of the frustrated antiferromagnetic Heisenberg model, for different lattice sizes, (a) $N=8$ and (b) $N=16$.

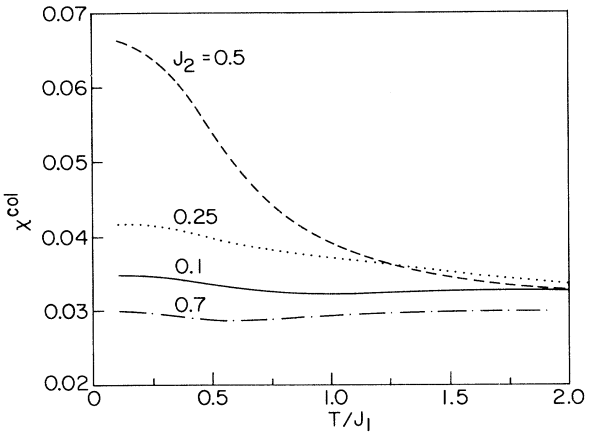

FIG. 7. Square of the column state order parameter, χ^{col} vs T.

Can we explain the behavior of $S(\mathbf{q})$ within the context of the dimer states?[22] In Fig. 8(a), we show the structure factor $S(\pi,\pi/2)$ for different values of the frustration parameter, while in Fig. 8(b), we present the results for $S(\mathbf{q})$ at $J_2/J_1=0.6$. We found that the largest value of $S(\pi,\pi/2)$ is reached in the intermediate region, and at $J_2/J_1\approx 0.6$, there is an almost perfect degeneracy between the structure factor for momenta (π,π), $(\pi,\pi/2)$, and $(\pi,0)$. Let us consider the state,

$$|\text{dimer}\rangle = |1\rangle + |2\rangle + |3\rangle + |4\rangle \ . \tag{12}$$

$|1\rangle$ denotes one possible column dimer state and the other three are obtained from $|1\rangle$ by translations and rotations in $\pi/2$. For a finite lattice, it is necessary to consider this combination (there is a finite probability for tunneling from one dimer to another), while in the thermodynamic limit, one dimer would be enough. Evaluating the structure factor in this state for $N=16$, we obtain[23]

$$S^{\text{dimer}}(\mathbf{q}) = \tfrac{1}{4}[1-E(\mathbf{q})] \ , \tag{13}$$

where

$$E(\mathbf{q}) = \tfrac{1}{19}[1+11(\cos q_x+\cos q_y)-(\cos q_x+\cos q_y)^2] \ . \tag{14}$$

In Table III, we compare the exact numerical results for $S(\mathbf{q})$ with the ones obtained from Eq. (13). The maximum value of $S(\mathbf{q})$ corresponds to momentum (π,π), while $(\pi,\pi/2)$ is enhanced with respect to the rest. In the limit of infinite temperature, since the spins are not correlated, all the structure factors have the common value $S(\mathbf{q})=\frac{1}{4}$, and, thus, for $\mathbf{q}=(\pi,\pi/2)$, there is an enhancement between $T=0$ and ∞. For $J_2/J_1=0.5$, the relative intensities of the structure factors for the different momenta are in qualitive agreement with those given by Eq. (13). However, as is shown in Fig. 9, the energy for this particular dimer configuration, Eq. (12), is not close to the exact ground-state energy. A better agreement in the energy at the intermediate region, at least for the 4×4 lattice, is obtained using an equal weight nearest-neighbor resonating valence bond state, $NN-RVB$, as is also shown in Fig. 9.

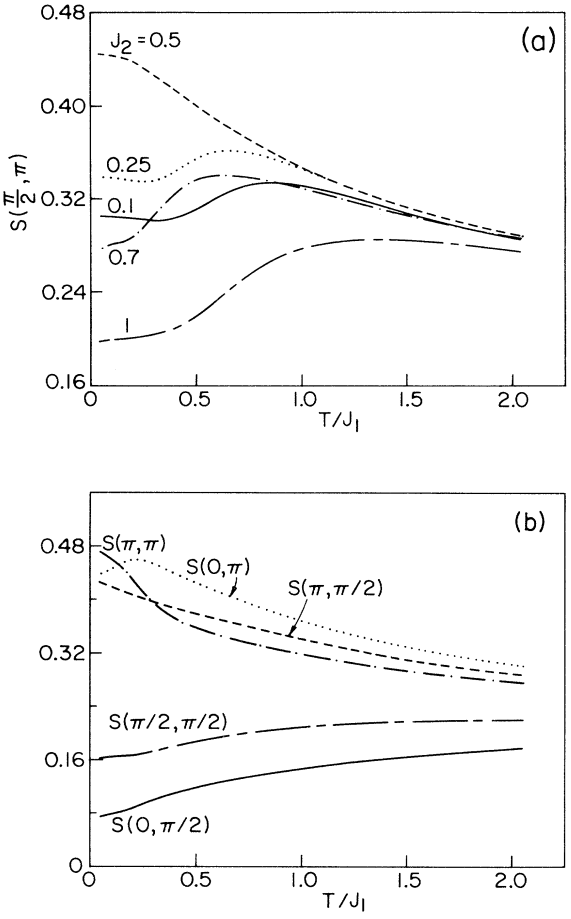

FIG. 8. (a) The structure factor $S(\pi,\pi/2)$ as function of temperature. (b) $S(\mathbf{q})$ vs T for $J_2/J_1=0.6$.

The corresponding values of $S^{RVB}(\mathbf{q})$, obtained using the $NN-RVB$ variational state are shown in Table III.[24] These results suggest that, at least for $T=0$ and $J_2/J_1\approx 0.5$, the $NN-RVB$ variational state can roughly explain the behavior of $S(\mathbf{q})$. For both the dimer and the $NN-RVB$ states, the enhancement of $S(\pi,\pi/2)$ over other values of $\mathbf{q}$ is related with the enhancement of short-distance correlations. Then, a qualitative description of the behavior of $S(\mathbf{q})$ at $J_2/J_1\approx 0.5$ seems to be possible using these variational states. Of course, note that this argument seems to be qualitative rather than quantitative and, thus, care must be taken in the analysis.

TABLE III. Structure factor at $T=0$. The numerical results correspond to $J_2/J_1=0.5$. In parentheses, we show the same quantity for $J_2/J_1=0.6$.

$\mathbf{q}$	$S(\mathbf{q})$	$S^{\text{dimer}}(\mathbf{q})$	$S^{RVB}(\mathbf{q})$
(π,π)	0.854 (0.469)	0.579	1.14
$(0,\pi)$	0.222 (0.429)	0.237	0.174
$(\pi/2,\pi/2)$	0.167 (0.164)	0.237	0.174
$(\pi/2,\pi)$	0.444 (0.426)	0.394	0.387
$(0,\pi/2)$	0.064 (0.077)	0.105	0.066

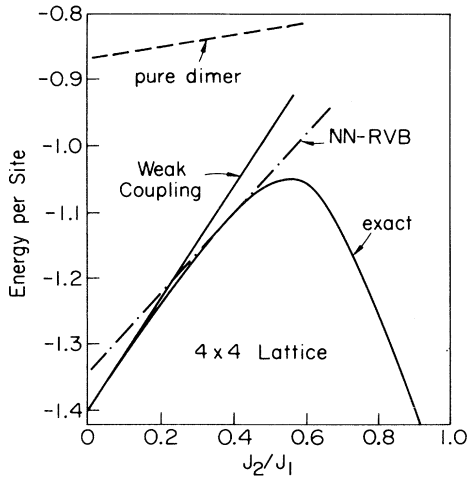

FIG. 9. Comparison of the ground-state energy as a function of J_2/J_1 with the energy of the dimer and $NN-RVB$ variational states. We also include the ground state energy in the weak coupling limit $J_2 \ll J_1$.

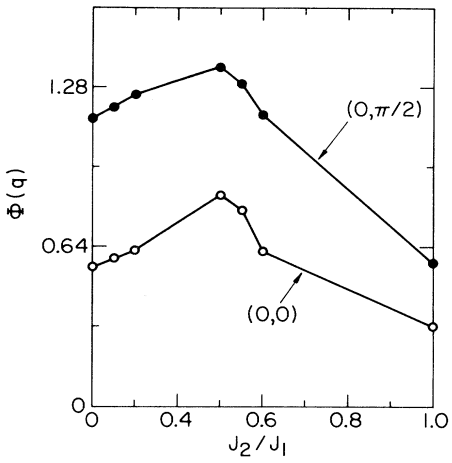

FIG. 10. Twisted susceptibility at $T=0$ as a function of J_2/J_1 at $\mathbf{q}=(0,0)$ and $(0,\pi/2)$.

It is clear that there is no room in these states to explain the quasidegeneracy observed in the structure factors at $J_2/J_1 \approx 0.6$. Also, note that we believe (although we have not done the calculation explicitly) that the RVB state cannot explain the enhancement in the dimer susceptibility found at intermediate values of frustration, and thus, we are not presenting it as a serious candidate for the ground state of the J_1-J_2 model. We are only pointing out that the other states besides the dimer can roughly explain the results for the structure factors.

Another state that as been proposed as a possible candidate for the ground state in the intermediate region of the FAFH is the *twisted* state. In the classical limit, it has been shown that twisted and spin order in the ground state in the intermediate region exist if exchange couplings at a distance of two lattice spacings are also considered.[10] The properties of the $J_1-J_2-J_3$ model have been analyzed using spin-wave techniques and numerical diagonalizations at $T=0$.[25] Even when the FAFH model Hamiltonian does not contain such a term as J_3 explicitly, it may appear as a result of thermal and quantum fluctuations as was pointed out in Ref. 11. The classical twisted state is different from the quantum mechanical twisted state, since the latter does not have spin order, only twisted order. Recently,[21] it has been found that the twisted order parameter changes very little with temperature showing that it is not enhanced with frustration, but simply less suppressed than in a Néel state. This calculation is very convincing, but we want to analyze this issue in more detail. For this purpose, we study at $T=0$ the twisted susceptibility,

$$\Phi(\mathbf{q})=\frac{1}{N}\sum_{i,j,\delta,\delta'} e^{i\mathbf{q}\cdot(\mathbf{i}-\mathbf{j})}\langle(\mathbf{S}_j\times\mathbf{S}_{j+\delta'})\cdot(\mathbf{S}_i\times\mathbf{S}_{i+\delta})\rangle \ . \quad (15)$$

This susceptibility measures the current-current spin correlation function in the xy plane. We generalize here previous calculations to the $\mathbf{q}\neq(0,0)$ case. In Fig. 10, we present our results. In the intermediate region, the twisted susceptibility at $\mathbf{q}=(0,\pi/2)$ is enhanced by a factor of 2 with respect to the infinite-temperature limit $\frac{3}{4}$ showing a maximum at $J_2/J_1 \approx (0.5-0.6)$. We do not have a simple explanation for these results. Clearly, a finite-size scaling analysis is needed to show if this maximum survives in the thermodynamic limit, but nevertheless, the twisted susceptibility at $\mathbf{q}=(0,\pi/2)$ cannot be discared using the infinite-temperature argument. Finally, we have not analyzed the uniform chiral order parameter,[11] since, at $T=0$, no indications of enhancement of this type of spin order have been found.

IV. SUMMARY

We have studied finite-temperature properties of the spin-$\frac{1}{2}$ frustrated antiferromagentic Heisenberg model on a square lattice using an exact diagonalization technique, which is based on the Lanczos algorithm. We have calculated static properties, such as specific heat, uniform susceptibility, spin-spin correlation functions in momentum space, and the corresponding susceptibility of the dimer order parameter. The study of the 4×4 lattice shows an enhancement at low temperatures, in the appropriate region of parameter space, both in $S[(\pi/2),\pi]$ and in the column operator (which indicates dimer order). While the enhancement of this structure factor can be explained by a dimer state, the results at $J_2/J_1 \approx 0.6$ (a near degeneracy of many structure factors) remain a puzzle. Nevertheless, we agree with Ref. 21 that the dimer state is a very strong candidate for the ground state of the FAFH in the intermediate region of frustration.

We have also calculated the twisted susceptibility at $T=0$ and *nonzero* $\mathbf{q}$, finding in the intermediate region an enhancement of this quantity for both $\mathbf{q}=(0,0)$ and $\mathbf{q}=(0,\pi/2)$. The possibility of a nonuniform twist has not been considered before in the literature, to the best of our knowledge. At $T=0$, for $J_2/J_1 \approx 0.6$ and $\mathbf{q}=(0,\pi/2)$, there is an enhancement of a factor of 2 with respect to the infinite-temperature limit, contrary to what

happens for $\mathbf{q}=(0,0)$, where the twisted susceptibility has no appreciable change in all the temperature range. Thus, we believe that the possible existence of twisted order in this model is not completely ruled out as implied by Ref. 21.

With respect to a possible phase transition at finite temperature in the intermediate region of the coupling parameters, our results indicate a sharpening of the specific heat in the region of interest. However, a studying only small systems, we cannot show convincingly if this peak will diverge in the thermodynamic limit.

ACKNOWLEDGMENTS

We thank R. R. P. Singh for useful correspondence and R. M. Martin for a critical reading of the manuscript. This project was supported by the National Science Foundation Grant Nos. DMR 8612860, STC 8809854, and PHY89-04035, supplemented by funds from the National Aeronautics and Space Administration. The computer simulations were done on a VAX 6410 and 6310 at the Material Research Laboratory. We acknowledge the use of its computational facilities.

*Also at Institute for Theoretical Physics, University of California at Santa Barbara, Santa Barbara, CA 93106.

[1]J. G. Bednorz and K. A. Muller, Z. Phys. B **64**, 189 (1986).

[2]P. W. Anderson, Science **235**, 1196 (1987); T. M. Rice, Z. Phys. B **67**, 141 (1987), and references therein; P. W. Anderson, Phys. Rev. Lett. **59**, 1497 (1987), and references therein.

[3]S. Chakravarty, B. I. Halperin, and D. R. Nelson, Phys. Rev. B **39**, 2344 (1989).

[4]M. Inui, S. Doniach, and M. Gabay, Phys. Rev. B **38**, 6631 (1988).

[5]J. D. Reger and A. P. Young, Phys. Rev. B **37**, 5978 (1988); M. Gross, E. Sanchez-Velasco, and E. Siggia, *ibid.* **39**, 2484 (1989); N. Trivedi and D. Ceperley, *ibid.* **40**, 2737 (1989).

[6]D. Mermin and H. Wagner, Phys. Rev. Lett. **17**, 1133 (1966).

[7]P. Chandra and B. Doucot, Phys. Rev. B **38**, 9335 (1988).

[8]N. Read and S. Sachdev, Phys. Rev. Lett. **62**, 1694 (1989).

[9]M. Gelfand, R. Singh, and D. Huse, Phys. Rev. B **40**, 10 801 (1989).

[10]P. Chandra, P. Coleman, and A. Larkin, Phys. Rev. Lett. **64**, 88 (1990).

[11]X. G. Wen, F. Wilczek, and A. Zee, Phys. Rev. B **39**, 11 413 (1989); V. Kalmeyer and R. B. Laughlin, Phys. Rev. Lett. **59**, 2095 (1987).

[12]E. Dagotto and A. Moreo, Phys. Rev. B **39**, 4744 (1989); Phys. Rev. Lett. **63**, 2148 (1989).

[13]F. Figueirido *et al.*, Phys. Rev. B **41**, 4619 (1989).

[14]J. Oitmaa and D. D. Betts, Can. J. Phys. **56**, 897 (1978).

[15]The ground state of the Heisenberg model on a 32-site lattice has been recently obtained [E. Dagotto *et al.* (unpublished)]. The energy per site for $J_2=0.0$ and $J_1=1.0$ is $-0.680\,179\,2$.

[16]D. Poilblanc, E. Gagliano, S. Bacci, and E. Dagotto (unpublished).

[17]E. Gagliano *et al.*, Bull. Am. Phys. Soc. **35**, 757 (1990).

[18]E. Gagliano and S. Bacci, Phys. Rev. Lett. **62**, 4154 (1989).

[19]E. Dagotto and A. Moreo, Phys. Rev. D **31**, 865 (1985); E. Gagliano, E. Dagotto, A. Moreo, and F. Alcaraz, Phys. Rev. B **34**, 1677 (1986); E. Gagliano and S. Bacci, Phys. Rev. D **36**, 546 (1987).

[20]G. Gomez-Santos, J. D. Joannopoulus, and J. W. Negele, Phys. Rev. B **39**, 4435 (1989).

[21]R. Singh and R. Narayanan, Phys. Rev. Lett. **65**, 1072 (1990).

[22]We thank R. Singh for useful conversations regarding this calculation.

[23]The dimer states are nonorthogonal, therefore, the overlap between them must be considered properly. In fact, the nonorthogonality of the dimer states gives second- and third-neighbors contributions to the structure factor. This is the origin of the third term in Eq. (14). The factor $\frac{1}{19}$ comes from the norm $\langle \text{dimer}|\text{dimer}\rangle = 19\times(2^8/4)$. For a calculation of matrix elements between dimer states, see S. Liang *et al.*, Phys. Rev. Lett. **61**, 365 (1988).

[24]We compute $S^{RVB}(\mathbf{q})$ writing explicitly the structure factor in terms of spin-spin correlation functions G_r and using for them the values calculated by M. Kohmoto, Phys. Rev. B **37**, 3812 (1988).

[25]A. Moreo, E. Dagotto, T. Jolicoeur, and J. Riera, Phys. Rev. B **42**, 6283 (1990).